2. P. Banerjee and R. Butterfield, Boundary Element Methods in Engineering Science, McGraw-Hill, New York (1982).
3. D. Colton and R. Kress, Integral Equations Methods in Scattering Theory [Russian translation], Mir, Moscow (1987).

PLASTIC MACRODEFORMATION WITH TWISTING UNDER PRESSURE FOR ALUMINUM WITH LOCALLY INTRODUCED GRAPHITE POWDER

V. V. Neverov

UDC 529.37

A description of plastic deformation of crystalline solids is given within the scope of dislocation theory and solid mechanics. Physical theories which describe microdeformation do not give a straightforward representation of a body as a whole since they cannot describe macrodeformation. The problem of combining these theories can only be solved taking account of the hierarchy of the scale levels for deformation [1]. The combination is supported by a weak experimental study of macroscopic deformation levels. As a rule deviation of macroscopic movements from laminar paths predicted by solid mechanics is small with normal plastic deformation schemes. Therefore in order to observe them methods are required which make it possible not only to carry out recording in large fields, but also quite fine fields [2]. However, another way is possible, i.e., by increasing the level of plastic deformation and property inhomogeneity for specimens. Development of macromovements is strengthened, which simplifies observing them. Macromovements and convective mass transfer in short cylindrical specimens of aluminum containing locally introduced graphite powder with plastic deformation in twisting under pressure are described and discussed. The study is also of interest in connection with the problem of preparing alloys by means of plastic deformation [3].

Study Procedure. Tests were performed in a "shear under pressure" device [3] with a restraining ring which made it possible to increase specimen thickness h to 3 mm with a piston diameter of 2R = 8 mm. After prior compression holes were drilled in the specimen parallel to the axis of rotation and they were filled with graphite powder with a particle size <0.5 mm. In other tests the powder was distributed in a thin layer within a specimen over a surface perpendicular to the axis of rotation. Then the cell was closed by the piston, a compressive pressure of 1 GPa was applied, and the piston was rotated to the prescribed number of rotations n. The rate of piston rotation $\dot{\varphi} = 0.14$ sec^{-1} which excluded specimen heating [4]. In order to provide parallelness for the specimen ends all of the device component surfaces transmitting a compressive force were ground for parallelness from both sides. Both cylinders, i.e., the cylinder with the piston and the cylinder at the end of which the specimen was placed in the restraining ring, were located in a guidance housing. The diameter of the housing exceeded that of the cylinders by not more than $a = 4\cdot10^{-2}$ mm. During tests the housing could rotate freely and therefore the slope of the cylinder axes did not exceed $\alpha = 2a/H \approx 2\cdot10^{-3}$, where H is cylinder height. Microsections were prepared from deformed specimens, the position of the graphite in them was observed from which material movement was assessed, and the microhardness was measured. Macromovements were compared with those calculated for a viscoplastic material model.

Results of Observations. In the first piston rotations with n < 10 a column of graphite was transformed into a screw-shaped band and from its pitch the distribution of displacements through the specimen thickness was found (Fig. 1a, n = 8, graphite in one hole ∅ = 1 mm at a distance from the axis r_0 = 3 mm; Fig. 1b, the same as for 1a but before introducing the graphite the aluminum was deformed with n = 20; all photographs magnified by eight).

Novokuznetsk. Translated from Zhurnal Prikladnoi Mekhaniki i Tekhnicheskoi Fiziki, No. 1, pp. 98-103, January-February, 1991. Original article submitted April 18, 1989; revision submitted July 20, 1989.

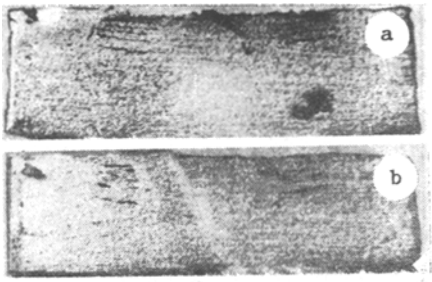

Fig. 1

From the equilibrium equation on cylindrical coordinates [5]

$$\frac{\partial \tau_{z\theta}}{\partial z} + 2\frac{\tau_{r\theta}}{r} + \frac{\partial \tau_{r\theta}}{\partial r} = 0 \qquad (1)$$

for a viscoplastic material with

$$\tau_{z\theta} = \tau_y + 2\eta\dot{\varepsilon}_{z\theta}, \ \tau_{r\theta} = \tau_y + 2\eta\dot{\varepsilon}_{r\theta} \qquad (2)$$

with normal notation for the coordinate axes, stress tensor components, and relative strain rate, τ_y is yield strength, η is viscosity coefficient, and by using the relationship

$$2\dot{\varepsilon}_{r\theta} = \frac{\partial v_\theta}{\partial r} - \frac{v_\theta}{r}, \ 2\dot{\varepsilon}_{z\theta} = \frac{\partial v_\theta}{\partial z}, \qquad (3)$$

we obtain

$$\frac{\partial^2 v}{\partial z^2} + \frac{\partial^2 v}{\partial r^2} + \frac{\partial v}{r\,\partial r} - \frac{v}{r^2} = -\frac{2\tau_y}{\eta}\frac{1}{r}, \qquad (4)$$

where $v \equiv v_\theta$ is tangential velocity of points. Equation (4) is solved with the boundary conditions

$$r = R, \ v = 0; \ z = 0, \ v = 0; \ z = h, \ v = r\dot{\varphi}. \qquad (5)$$

In omitting the operation of the solution it is noted that the substitution

$$v\,(r,\ z) = \mathcal{R}\,(r)(\mathcal{E}\ \mathrm{ch}\,kz + \mathcal{L}\ \mathrm{sh}\,kz) \qquad (6)$$

separates variables in the homogeneous equation corresponding to (4) after which the equation with r by substituting y = kr is transformed into a Bessel equation.

The experimental distribution of displacements over the specimen height is more nonuniform than the calculated distribution, and higher than that calculated in the region adjacent to the piston. Since aluminum strengthens in the course of deformation (in view of which it might be possible to expect a more uniform distribution than the calculated one), then the cause whose action with small n overlies the strengthening effect is connected with graphite. Whence it follows that over the surface of graphite location resistance to shear is reduced, and over it there is partial sliding.

Random irregular plastic movements erode the graphite plane, and with $n \geq 15$ they merge into a cloud (Fig. 2, two symmetrical holes $\varnothing = 1$ mm with graphite, $r_0 = 3$ mm, graphite content 2 vol. %; a) n = 50, c) n = 150, e) n = 100). At first the cloud forms close to the piston. Material microhardness in the cloud becomes higher than that in the surrounding area (for n = 50 the cloud microhardness is 0.7 GPa, and outside the cloud it is 0.4 GPa), and consequently the graphite starts to act as a strengthening addition. Therefore, gradually the cloud forms in the more distant layers from the piston. After a relatively uniform distribution of graphite a layered structure is created and light interlayers with a lower graphite content development (Fig. 1b). Starting from n = 5 in specimens there is development of macroscopic rotational movement when material from the central part of the layers in which deformation is concentrated is squeezed out primarily beneath the piston (the material

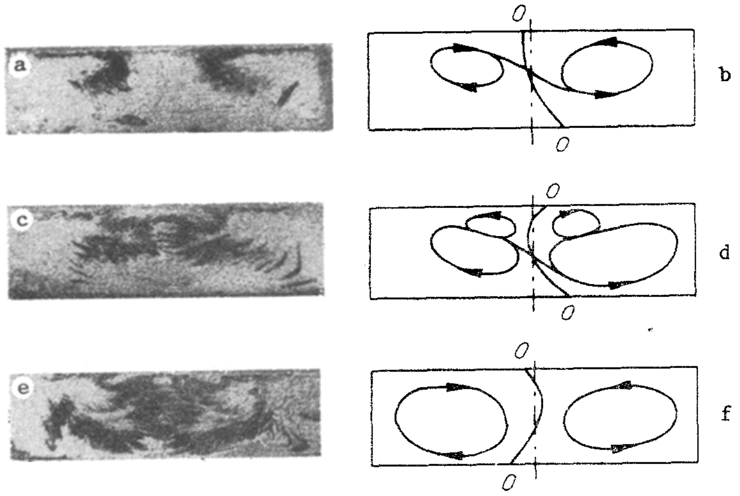

Fig. 2

movement scheme is shown by arrows in Fig. 2). Before merging of the converging parts of the cloud bridges of material interlayers with graphite form between them (Fig. 2c). The structure and shape of the clouds does not correspond to axial symmetry. Deviation of the twisting axes constructed from the position of graphite (Fig. 2, 00) from the geometric axis reaches 1 mm. Axial symmetry of equal displacement surfaces is disturbed.

With an increase in the amount of graphite introduced the mixing process accelerates both as a result of an increase in the amplitude of regular macrorotational movement, and due to reinforcement of random movements (Fig. 3, two symmetrical holes $\varnothing = 1.5$ mm, $r_0 = 3$, graphite content 4.5 vol. %; a-d) n = 100, 150, 250, 300).

After distribution of the graphite almost throughout the deformed volume accompanied by material strengthening (for example with 4.5% graphite the microhardness increases to 0.9 GPa), a layered axisymmetrical structure forms in the specimen (see Fig. 3). Graphite particles are broken down, they become less than the wavelength of visible light, and therefore they are invisible and the microsection lightens.

If the aluminum is plastically deformed by twisting prior to introducing the graphite, then the screw-shaped band of graphite does not form. Graphite is distributed by inclusions (Fig. 1b) whose size, shape, mutual position, and inclination are irregular, although there are signs of a screw-shaped band. This irregularity is reinforced with an increase in the degree of prior material deformation. These observations show that plastic deformation promotes localization of shears. In fact, the shear surface separates the band of graphite into inclusions. Since the degree of deformation which occurs in the continuously distributed shears decreases, there is also a decrease in stretching, and therefore the thickness of inclusions is greater than the thickness of the band. Shear localization surfaces are not axisymmetrical. As a result of this there is development of local rotational movements [6] which disturb conformity between the position of inclusions and the band. Prior deformation prevents development of regular macrorotational movement. Cloud formation is prolonged to $n \approx 100$.

It is natural to assume that the macroscopic deviations described above in the position of the graphite from axisymmetrical and the process of cloud formation are also connected with random rotational movements but of a greater or lesser scale.

Thus, there are regular and random rotational movements. These movements are stimulated by the presence of graphite and they fade with large deformations.

If the graphite is arranged within a specimen in the form of a thin layer perpendicular to the axis of rotation, then with twisting from this surface in the shear direction thin layers of aluminum are drawn out, i.e., tongues. It is possible to observe them if after a small amount of deformation a specimen is divided along the surface of graphite location (Fig. 4).

<u>Discussion of Observations.</u> Macrorotational regular movement may be explained by two causes: rocking of the piston which is created with rotation as a result of the nonparallel-

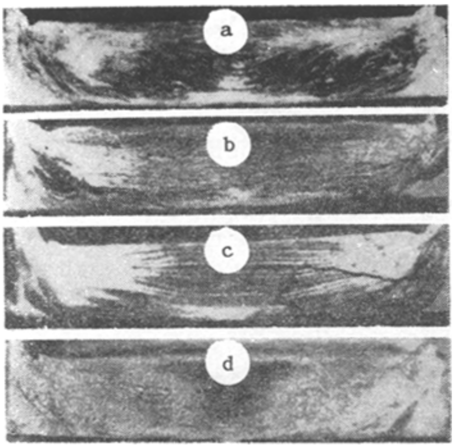

Fig. 3

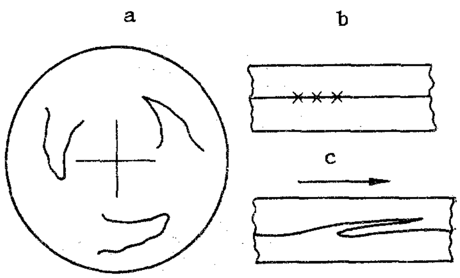

Fig. 4

ness of the end surfaces of a specimen, and by the compressive effect of twisted material. We calculate the drop in stresses created at the center and at the edge of a specimen in both cases. For the first cause since α is the maximum possible angle of inclination, $\Delta\sigma_z = E0.6\Delta hh^{-1} \leq E0.6\alpha h^{-1} \approx 0.16$ GPa. Here $E = 7\cdot10^2$ GPa is aluminum elasticity modulus; Δh is piston edge displacement without taking account of its deformation; coefficient 0.6 takes account of piston deformation.

With twisting of a cylindrical layer with radius r and thickness dr as a result of stretching the generating line in a layer tensile stresses σ also operate along a stretched fiber, i.e., linear stress $dT = \sigma dr$. Laplace compressive pressure is created $d\sigma = R_f^{-1}dT = R_f^{-1}\sigma dr$ (R_f^{-1} is radius of curvature of a stretched fiber). Since $R_1^{-1} + R_2^{-1} = \text{const}$, $R_{1,2}$ is radius of curvature of the surface in mutually perpendicular sections, then for cylindrical surface $R_f^{-1} = r^{-1} - R_e^{-1}$, where R_e is radius of curvature of an ellipse at the point of intersection with a short semiaxis. An ellipse is obtained in a section of a cylinder with a plane perpendicular to the stretched fiber. Whence $R_e = r\cos^2\beta$ and $R_f = r\sin^2\beta$ (β is angle of inclination of the plane of a section to the end plane of the cylinder). Then $d\sigma_r = \sigma\sin^2\beta r^{-1}dr$. Since in tests the whole of a specimen is in a plastic condition, then σ equals the yield strength σ_y and $\beta = \gamma$, i.e., the elastic relative shear strain for a cylindrical layer. For the greatest elastic deformation $\beta = \gamma \approx 0.05 \ll 1$, $\sin^2\beta \approx \beta^2$, and

$$\Delta\sigma_r \approx \sigma_y \beta^2 \ln R/r_1. \tag{7}$$

By taking $r_1 = 0.3$ mm (see Fig. 1) we obtain $\Delta\sigma_r \approx 7\cdot10^{-3}\,\sigma_y$, which is very small and it relates to the lower part of the specimen. If a fiber of the material is inclined a little to the end plane (see Fig. 1), then $\beta = \pi/2$, $\Delta\sigma_r \approx 2.5\,\sigma_y$. For annealed aluminum $\sigma_y = 0.07$ GPa and $\Delta\sigma_r = 0.18$ GPa, for work-hardened aluminum $\sigma_y = 0.15$, $\Delta\sigma_r = 0.37$ GPa, and for a mixture strengthened with graphite $\sigma_y = 0.3$, $\Delta\sigma_r = 0.75$ GPa.

The high value and more favorable direction of stresses in the second case is noted. With an increase in the amount of graphite the material becomes stronger, which should weaken macrorotational movement if it is caused by rocking of the piston. In fact, the reverse is observed. Piston rocking causes a change in thickness at the specimen edge of not more than $0.6R\alpha \approx 5\cdot10^{-3}$ mm. Random deviations of the twisting axis from the geometric axis are one to two orders greater. It is difficult to suggest that the action of rocking developed on a background of much higher random deviations. This makes it possible to confirm that the main reason for macrorotational movement is radial compression.

A condition for development of this effect is continuous distribution of shears. If they are localized in individual surfaces, then fibers are cut up and compression does not occur. Shear localization is explained by absence of macrorotation in specimens after considerable deformation. However, this movement fades gradually, and this depends on the position of the graphite. Appearance in a cloud of interlayers with a small graphite content (similar to the condition with tests whose results are reflected in Fig. 4a) makes it possible to confirm that with shear along individual surface tongues form in the cloud along these surfaces. With an increase in deformation the thickness of the screw-shaped graphite band decreases. Where band continuity is disturbed a layer of aluminum is captured and under sliding conditions in neighboring areas where the band is retained tongues form (Fig. 4b; areas of capture are marked with crosses) [6]. Here in a cloud material from neighboring regions with a low graphite content is drawn in. Tongues are stretched fibers which after shear localization create a compressing effect. Tongue formation leads to a change in the position of the shear localization surfaces, and therefore the whole of the upper part of the specimen is worked plastically. Only after a reduction in the size of areas with layered placing of graphite does tongue formation and macrorotational movement cease. A layered axisymmetrical macrostructure forms in specimens.

Prior deformation eliminates the stage of laminar movement. Graphite is located not along a surface, but as individual inclusions, and therefore neither tongues form nor is there macrorotational movement.

As a result of random deviations of the twisting axis from the geometrically correct position of the point trajectories for volumes separated by a shear surface, they have a spiral nature with respect to each other. As a result of this transfer of graphite is created along shear surfaces in the radial direction, which explains formation of bridges between converging parts of the cloud.

Thus, the observations are explained by regular rotational movement caused by compression of twisted material and random rotations. In a random rotation, and more so in a regular rotation, a considerable number of grains are drawn in, and therefore the effect of these movements of crystallographic features of plastic deformation micromechanisms may be ignored. Evolution of movement and the macrostructure is determined by two tendencies: deformation strengthening of the material increases the localization macroshears; the degree of inhomogeneity caused by presence of graphite passes through a maximum. The structures observed are dissipative and self-limiting [7], and each preceding structure prepares the system for formation of the next. Regular macrorotation is a specific feature of the twisting scheme, whereas random rotations are movement which is of a general nature for inhomogeneous specimens. Whence combined macro and micro-description of plastic deformation requires development of a theory for random macromovements and the synergetic macrostructures which arise. A model for the basic disturbed laminar flow for random movement is illustrated in Fig. 4.

In obtaining alloys by means of plastic deformation the original material is a mixture of powder components. The intensity of random rotational movement is determined by inhomogeneities connected with the difference in properties and reaction of particles, and also the position of the components. Rotations promote a breakdown and increase in the contact area for components, and consequently the kinetics of the process are accelerated. Whence increased inhomogeneity, e.g., the friction coefficient between particles, may accelerate the process. It is not ruled out that this effect was observed in [8] with addition of toluol to mechanically alloyed powders. Finally, tests showed that a layered arrangement of components in the initial stages of the process promotes mixing.

LITERATURE CITED

1. V. E. Panin, V. A. Likhachev, and Yu. V. Grinyaev, Structural Levels of the Deformation of Solids [in Russian], Nauka, Novosibirsk (1985).
2. V. E. Panin, L. B. Zuev, V. I. Danilov, and N. M. Mnikh, "Features of the displacement field with plastic deformation of coarse-grained silicon iron," Fiz. Met. Metalloved., 66, No. 5 (1988).
3. V. V. Neverov, V. N. Burov, and A. I. Korotkov, "Features of diffusion processes in the plastic deformation of a mixture of zinc and copper," Fiz. Met. Metalloved., 46, No. 5 (1978).
4. V. N. Burov, P. P. Zhitnikov, V. V. Neverov, and V. G. Suppes, "Nature of compressed thin layer explosions," Zh. Prikl. Mekh. Tekh. Fiz., No. 4 (1986).
5. L. N. Kachanov, Bases of Plasticity Theory [in Russian], Nauka, Moscow (1969).
6. V. V. Neverov and P. P. Zhitnikov, "Rotational movements of material with shear plastic deformation of thin layers," Izv. Vyssh. Uchebn. Zaved. SSSR, Fiz., No. 2 (1989).
7. H. Haken (ed.), Synergetics – A Workshop. Proceedings of the International Workshop on Synergetics at Schloss Elman, Bavaria, Germany, May 2-7, 1977, Springer-Verlag (1977).
8. B. P. Dolgin, M. A. Vanek, T. McGory, and D. J. Ham, "Mechanical alloying of Ni, Co, and Fe with Ti. Formation of amorphous phase," J. Non-Cryst. Solids, 87, No. 3 (1986).